Journal of Engineering Mathematics 19 (1985) 3–19.

A new method for the numerical solution of the Reynolds equation for gas-lubricated slider bearings

M.C. PANDIAN

Department of Mathematics, University of Alabama, University, AL 35486, USA

(Received January 12, 1984)

Summary

The steady-state Reynolds equation for gas lubricating films leads to a quasilinear boundary-value problem in two dimensions. This equation contains a first-order derivative term whose coefficient is nonlinear and also large for most of the practical cases. Thus, this becomes a quasilinear singular perturbation problem. Existing numerical schemes are faced with the failure of convergence as well as numerical instability which often results in overshooting the answers. Asymptotic approximations also give poor results if the film-thickness ratios are not small. In this paper an accurate and reliable numerical scheme is presented. Convergence is proved independent of the bearing numbers and film-thickness ratios. A weighted upwind-difference form is used to discretize the differential equation. Theory of M-matrices and associated inequalities are employed to prove the ensuing monotonicity. The analysis presented in this paper can be extended to a more general class of singular-perturbation quasilinear boundary-value problems. Numerical results and graphs for pressure distributions and bearing loads are provided for the parabolic slider. Comparisons are made with other existing results concerning numerical as well as asymptotic analysis.

1. Introduction

The most commonly encountered problem in lubrication technology is that of producing data (pressure distributions, resulting forces and moments, friction power losses) for steady-state operation of gas-bearing systems. Once the pressure distribution has been obtained, it is easy to evaluate other data. The steady-state Reynolds equation for the pressure $p(\xi, \eta)$ at a point (ξ, η) in a compressible lubricating film is

$$\frac{\partial}{\partial \xi}\left[\left(h^3 p^{1/n}\frac{\partial p}{\partial \xi}\right)/\mu\right]+\frac{\partial}{\partial \eta}\left[\left(h^3 p^{1/n}\frac{\partial p}{\partial \eta}\right)/\mu\right]=6U\frac{\partial}{\partial \eta}\left(hp^{1/n}\right) \tag{1.1}$$

where μ is the viscosity, U is the effective surface velocity, $h = h(\xi, \eta)$ the film thickness, η is the coordinate direction in which the slider is moving, and n is the exponent in the polytropic gas law

$$p\rho^{-n} = \text{constant}. \tag{1.2}$$

The problem is to solve (1.1) over a rectangular region with boundary lines $\xi = L/2$, $\xi = -L/2$, $\eta = 0$, and $\eta = B$. Here, L and B represent the length and breadth of the film, respectively. The film-thickness function is taken to be symmetric, $h(\xi, \eta) = h(-\xi, \eta)$.

Since this symmetry implies a symmetry in the pressure function, $p(\xi, \eta) = p(-\xi, \eta)$, it suffices to consider only the upper half of the rectangle. This symmetry implies the boundary condition $\partial p/\partial \xi(0, \eta) = 0$. The other boundary conditions are $p(\xi, 0) = p_a$, $p(\xi, B) = p_a$, and $p(L/2, \eta) = p_a$, where p_a represents the ambient pressure.

With gaseous lubricant and metallic materials, the fluid film is essentially isothermal. Thus for most gases, viscosity can be regarded as a constant and n is taken as 1 in (1.2). Equation (1.1) can be made dimensionless by normalizing all the variables with appropriate reference quantities. That is, $P = p/p_a$, $L' = L/B$ (slenderness ratio), $x = \xi/B$, $y = \eta/B$, $H = h/h_m$, and $\Lambda = 6\mu UB/(h_m^2 p_a)$ where h_m is the minimum film thickness in the sliding direction. Thus (1.1) becomes

$$\frac{\partial}{\partial x}\left(H^3 P \frac{\partial P}{\partial x}\right) + \frac{\partial}{\partial y}\left(H^3 P \frac{\partial P}{\partial y}\right) = \Lambda \frac{\partial}{\partial y}(PH), \tag{1.3}$$

where Λ is called the Reynolds number or bearing number. The boundary conditions are $P(x, 0) = 1$, $P(x, 1) = 1$, $P(L'/2, y) = 1$, and $\partial P/\partial x(0, y) = 0$ for $0 \leqslant x \leqslant L'/2$, $0 \leqslant y \leqslant 1$. the y-coordinate gives the direction in which the slider is moving. For more details, see [1], Ch. 1. In view of the difficulties encountered by purely analytical methods in dealing with the nonlinear nature of (1.3), the application of numerical methods to gas-bearing problems is of great importance. Further, it is noted in [1], pp. 188, that, "in fact, physical experimentation is so difficult that experimentation with a computer is likely to be more practical". Thus, it is important to have a reliable, economical and stable (accurate) numerical scheme. In this paper, such a scheme will be presented. The existing iterative techniques [1, Ch. 7; 2, 3] are hit-or-miss type. That is, success (convergence) of these schemes are not *a priori* known and their behaviours are very disappointing, especially when the Reynolds numbers and the film-thickness ratios are large. In fact, it is remarked in [3] that, "the convergence characteristics of these iteration techniques are difficult to analyse and skill and past experience are the most valuable guides in this field". The existing schemes are not only faced with the failure of convergence, but also they show numerical instability which often results in overshooting the answer. Thus, the credibility of the computed values with such unstable schemes is questionable. For more detailed discussion, see Section 3. The new iterative technique presented in this paper is numeri-

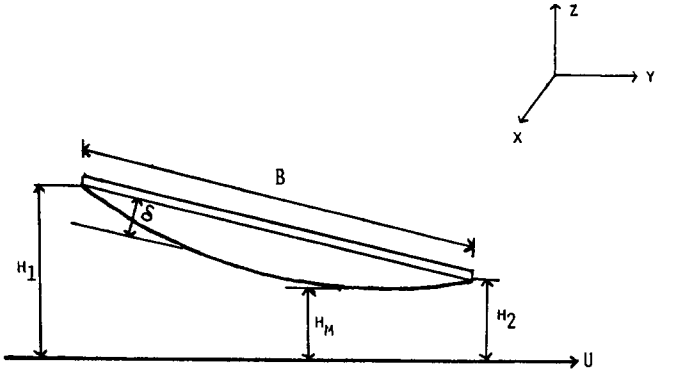

Figure 1. Curved slider bearing with crown hight δ. Normalized quantities are $H = h/h_2$, $H_1 = h_1/h_2$ (film-thickness ratio), and $\beta = \delta/h_2$; $\epsilon = H_1 - 1$ is referred as the eccentricity.

cally stable, and the convergence of iterations is proved independent of Reynolds numbers and film-thickness ratios.

The bearing shapes considered here are plane, cylindrically curved, and spherically curved. Particular nomenclature for the curved slider is shown in Fig. 1. The crown height, δ, is measured at the geometric center and it is positive for convex and negative for concave sliders. The film thickness functions for various geometries are given below.

For longitudinal cylindrical pads,

$$H(y) = H_1 - (H_1 - 1)y + 4\beta y(y-1). \tag{1.4}$$

For transversely crowned pads,

$$H(x, y) = H_1(1-y) + y + \frac{4\beta x^2}{L'^2}. \tag{1.5}$$

For spherically crowned pads,

$$H(x, y) = H(1-y) + y + 2\beta\left[y(y-1) + \frac{x^2}{L'^2}\right]. \tag{1.6}$$

The derivation of these expressions and other details can be found in [1], pp. 197-200. In the case of an infinitely long slider bearing, the following parabolic film shape is considered [4],

$$H(y, \epsilon, a) = 1 + \epsilon\left[ay^2 - (1+a)y + 1\right], \tag{1.7}$$

where $1 + \epsilon = H_1$ is the film-thickness ratio, and a is the curvature.

In Section 2 the numerical scheme is given. Computed results for selected examples as well as comparisons with other schemes are presented in Section 3.

2. Numerical procedure

Under the transformation $u = P^2H^2$, the Reynolds equation (1.3) becomes

$$-H(x, y)\left(\frac{\partial^2 u}{\partial x^2} + \frac{\partial^2 u}{\partial y^2}\right) + \frac{\partial H}{\partial x}\frac{\partial u}{\partial x} + \frac{\partial H}{\partial y}\frac{\partial u}{\partial y} + 2\left(\frac{\partial^2 H}{\partial x^2} + \frac{\partial^2 H}{\partial y^2}\right)u + \frac{\Lambda}{\sqrt{u}}\frac{\partial u}{\partial y} = 0 \tag{2.1}$$

with boundary conditions $u(x, 0) = H^2(x, 0)$, $u(x, 1) = H^2(x, 1)$, $u(L/2, y) = H^2(L/2, y)$, and $\partial u/\partial x(0, y) = 0$. We set up a grid: $x_i = i\Delta x$, $y_j = j\Delta y$ with $(M+1)\Delta x = L/2$ and $(N+1)\Delta y = 1$. The diffusion term $\Delta^2 u = \partial^2 u/\partial x^2 + \partial^2 u/\partial y^2$ is discretized using the standard five-point difference scheme. The first-order derivative terms in the linear part of (2.1) are approximated using centered differences. The nonlinear term is approximated as

$$\left.\frac{\Lambda u_y}{\sqrt{u}}\right|_{i,j} \approx \frac{\Lambda}{\sqrt{u_{i,j}}}\frac{\Delta u_{i,j}}{\Delta y},$$

$$\Delta u_{i,j} = \frac{1-\alpha}{2}u_{i,j+1} + \alpha u_{i,j} - \frac{1+\alpha}{2}u_{i,j-1}, \tag{2.2}$$

where $u_{i,j} = u(x_i, y_j)$ and α, $0 \leqslant \alpha \leqslant 1$, is the coefficient of upwind differencing which will be decided later. Notice that $\alpha = 0$ corresponds to the centered-difference approximation, and $\alpha = 1$ leads to full upwind form. The resulting nonlinear system can be written as

$$Au + \Delta y \frac{\Lambda}{\sqrt{u}} \Delta u = b, \tag{2.3}$$

where b is the given vector determined by the boundary conditions, $u = (u_{i,j})$ is the unknown vector, and A is a non-singular $NM \times NM$ matrix which represents the linear part in (2.1). For the $(i,j)^{\text{th}}$ grid point, (2.3) gives

$$s(i,j)u_{i,j} + s_1(i,j)u_{i,j-1} + s_2(i,j)u_{i,j+1} + s_3(i,j)u_{i-1,j}$$
$$+ s_4(i,j)u_{i+1,j} + \Delta y \frac{\Lambda}{\sqrt{u_{i,j}}} \Delta u_{i,j} = 0,$$

where

$$\begin{aligned}
s(i,j) &= \left\{ 2H + \sigma 2H + 2(\Delta y)^2 \left(H_{xx} + H_{yy} \right) \right\} \Big|_{i,j}, \\
s_1(i,j) &= \left(-H - \frac{\Delta y}{2} H_y \right) \Big|_{i,j}, \\
s_2(i,j) &= \left(-H + \frac{\Delta y}{2} H_y \right) \Big|_{i,j}, \\
s_3(i,j) &= \left(-\sigma H - \frac{\sigma \Delta x}{2} H_x \right) \Big|_{i,j}, \\
s_4(i,j) &= \left(-\sigma H + \sigma \frac{\Delta x}{2} H_x \right) \Big|_{i,j}, \quad \text{and} \quad \sigma = \left(\frac{\Delta y}{\Delta x} \right)^2.
\end{aligned} \tag{2.4}$$

The normal derivative boundary condition is approximated as $u_{1,j} = u_{0,j}$ $(j = 1, 2, \ldots, N)$. The coefficient of upwind differencing $\alpha_{i,j}$ is chosen so that

$$\frac{\Lambda}{\sqrt{u_{i,j}}} \Delta y \frac{(1 - \alpha_{i,j})}{2} \leqslant \left(H - \frac{\Delta y}{2} H_y \right) \Big|_{i,j},$$

that is,

$$\alpha_{i,j} \geqslant 1 - \frac{\left(2H - \Delta y H_y \right)_{i,j}}{\dfrac{\Lambda}{\sqrt{u_{i,j}}} \Delta y} \quad (i = 1, 2, \ldots, M; j = 1, 2, \ldots, N).$$

Let $\underline{u}$ be a lower solution of (2.3) (see the Appendix). Then, $\alpha_{i,j}$ is chosen as

$$\alpha_{i,j} = \max \left\{ 0, 1 - \frac{\left[\left(2H(x_i, y_j) - \Delta y H_y(x_i, y_j) \right) \sqrt{\underline{u}_{i,j}} \right]}{\Lambda \Delta y} \right\}$$

For convenience, delete the subscripts in α, and denote $f(u_{i,j}) = \Lambda\Delta y/\sqrt{u_{i,j}}$. Define $Q^{(k-1)}$, a block diagonal matrix, as

$$\begin{bmatrix} D_{N,1} & & \\ & \ddots & \\ & & D_{N,M} \end{bmatrix}$$

where $D_{N,i}$ is an $N \times N$ diagonal matrix $(w_{i,1}^{(k-1)}, \ldots, w_{i,N}^{(k-1)})$,

$$w_{i,j}^{(k-1)} = \max\left\{0, \left|f'\left(u_{i,j}^{(k-1)}\right)\right|\left[\frac{(1+\alpha)}{2}\bar{u}_{i,j-1} - \left(\alpha u_{i,j}^{(k-1)} + \frac{(1-\alpha)}{2}u_{i,j+1}^{(k-1)}\right)\right]\right\}. \quad (2.5)$$

Here, $\bar{u}$ is an upper bound for $u^{(k)}$. The construction of $\bar{u}$ will be discussed later.

To solve (2.3), the following iterative scheme is considered.

$$\begin{aligned} &Au^{(k)} + f(u^{(k-1)})\Delta u^{(k)} + Q^{(k-1)}u^{(k)} = b + Q^{(k-1)}u^{(k-1)}, \\ &u^{(0)} = \underline{u}, \qquad \text{for} \quad k = 1, 2, \ldots. \end{aligned} \quad (2.6)$$

Define, for $i = 1, 2, \ldots, M$; $j = 1, 2, \ldots, N$,

$$g^{(k-1)}(i,j) = s(i,j) + \alpha f\left(u_{i,j}^{(k-1)}\right) + w_{i,j}^{(k-1)},$$

$$g_1^{(k-1)}(i,j) = s_1(i,j) - \frac{(1+\alpha)}{2}f\left(u_{i,j}^{(k-1)}\right),$$

$$g_2^{(k-1)}(i,j) = s_2(i,j) + \frac{(1-\alpha)}{2}f\left(u_{i,j}^{(k-1)}\right),$$

$$g_3(i,j) = s_3(i,j),$$

$$g_4(i,j) = s_4(i,j),$$

where s, s_1, s_2, s_3 and s_4 are given by (2.4). Fix $i \in \{1, 2, \ldots, M\}$, and $j \in \{1, 2, \ldots, N\}$. With the above notations, (2.6) gives

$$g_1^{(k-1)}(i,j)u_{i,j}^{(k)} + g_1^{(k-1)}(i,j)u_{i,j-1}^{(k)} + g_2^{(k-1)}(i,j)u_{i,j+1}^{(k)} + g_3^{(k-1)}(i,j)u_{i-1,j}^{(k)}$$

$$+ g_4^{(k-1)}(i,j)u_{i+1,j}^{(k)} = 0,$$

where $u_{1,j}^{(k)} = u_{0,j}^{(k)}$, $u_{i,0}^{(k)} = H^2(x_i, 0)$, $u_{i,N+1}^{(k)} = H^2(x_i, 1)$, $u_{M+1,j}^{(k)} = H^2(L'/2, y_j)$.

Let $T^{(k-1)}$ be the following block tridiagonal matrix,

$$T^{(k-1)} = \begin{bmatrix} G_1 & S_1 & & & \\ R_2 & G_2 & S_2 & & \\ & \ddots & \ddots & \ddots & \\ & & & & S_{M-1} \\ & & & R_M & G_M \end{bmatrix},$$

$$G_1 = \begin{bmatrix} \tilde{g}(1,1) & g_2^{(k-1)}(1,1) & & & \\ g_1^{(k-1)}(1,2) & \tilde{g}(1,2) & g_2^{(k-1)}(1,2) & & \\ \ddots & \ddots & \ddots & & \\ & & & & g_2^{(k-1)}(1,N-1) \\ & & & g_1^{(k-1)}(1,N) & \tilde{g}(1,M) \end{bmatrix}_{N\times N},$$

$\tilde{g}(1,j) = g^{(k-1)}(1,j) - g_3(i,j)$ $(j = 1, 2, \ldots, N)$; for $i = 2, 3, \ldots, M$,

$$G_i = \begin{bmatrix} g^{(k-1)}(i,1) & g_2^{(k-1)}(i,1) & & & \\ g_1^{(k-1)}(i,2) & g^{(k-1)}(i,2) & g_2^{(k-1)}(i,2) & & \\ \ddots & \ddots & \ddots & & \\ & & & & g_2^{(k-1)}(i,N-1) \\ & & & g_1^{(k-1)}(i,N) & g^{(k-1)}(i,N) \end{bmatrix}_{N\times N},$$

$R_i = \text{diagonal}\ (g_3(i,1), \ldots, g_3(i,N))_{N\times N}$, and $S_i = \text{diagonal}\ (g_4(i,1), \ldots, g_4(i,M))_{N\times N}$ for $i = 1, 2, \ldots, M$.

Now, equation (2.6) can be rewritten as

$$T^{(k-1)}u^{(k)} = b + Q^{(k-1)}u^{(k-1)}. \tag{2.8}$$

Notice that if the slider is of infinite length then the second-derivative term with respect to x will be dropped in (1.3) and it becomes a problem in one dimension. In this case, $T^{(k-1)}$ is simply a tridiagonal matrix similar to G_i (without the i index).

By our choice of α, the coefficient of upwind differencing (2.4), it follows that $g_2^{(k-1)} \leqslant 0$. Since $\alpha \geqslant 0$, and the Reynolds number Λ in $f(u)$ will dominate the term $g_1^{(k-1)}$, one can obtain that $g_1^{(k-1)} \leqslant 0$. Notice that for film type (1.4), $H_x = 0$. In this case, it readily follows that g_3 and g_4 are nonpositive. For other film types, in practice, the normalized crown height will be small. Thus, in these cases also (if necessary, by properly choosing the grid), one can have that $g_3 \leqslant 0$ and $g_4 \leqslant 0$. So, the matrix $T^{(k-1)}$ is off-diagonally nonpositive. Further, whenever the normalized crown height $\beta \geqslant 0$, it is easy to check that

$$g^{(k-1)}(i,j) + g_1^{(k-1)}(i,j) + g_2^{(k-1)}(i,j) + g_3(i,j) + g_4(i,j) \geqslant 0.$$

In the other case also, since β is small in practice, one can see (if necessary, by choosing

$w_{i,j} \geqslant |2(\Delta y)^2(H_{xx}+H_{yy})|_{i,j}|$) that the same inequality is true. Hence, the matrix $T^{(k-1)}$ is diagonally dominant and off-diagonally nonpositive. Further, the lower triangular submatrix of $T^{(k-1)}$ is strictly diagonally dominant. Thus, by Theorem A.1 of the Appendix, $T^{(k-1)}$ is an M-matrix. That is, $T^{(k-1)}$ is inverse positive for $k = 1, 2, \ldots$.

Choose $\bar{u} = \max_{i,j}\{b_{i,j}\}$ for $i = 1, 2, \ldots, M$; $j = 1, 2, \ldots, N$. Notice that $\bar{u} \geqslant b$, and $\underline{u}$ is taken as $\underline{u} \leqslant \bar{u}$. Now, it will be shown that $\bar{u} \geqslant u^{(k)}$, for $k = 1, 2, \ldots$. To make the ideas clear for the proof of this part, consider the case $\beta \geqslant 0$ only. (For a complete discussion, see Section 2.2). By selection, $\bar{u} \geqslant \underline{u} = u^{(0)}$. Assume that $\bar{u} \geqslant u^{(k-1)}$. Since $Q^{(k-1)} \geqslant 0$, it follows that

$$T^{(k-1)}\bar{u} \geqslant b + Q^{(k-1)}\bar{u} \geqslant b + Q^{(k-1)}u^{(k-1)} = T^{(k-1)}u^{(k)}.$$

Thus, since $T^{(k-1)}$ is inverse positive, $\bar{u} \geqslant u^{(k)}$. By induction, one has $\bar{u} \geqslant u^{(k)}$, for $k = 1, 2, 3, \ldots$.

Next, the object is to prove the iterates $u^{(k)}$, $k = 1, 2, \ldots$, are monotonic increasing. Notice from (2.2) that, for any two vectors u and v, $\Delta u - \Delta v = \Delta(u - v)$. Since $u^{(0)} = \underline{u}$ is a lower solution (see the Appendix) one has

$$Au^{(0)} + f(u^{(0)})u^{(0)} \leqslant b. \tag{2.9}$$

So, it follows, by taking $k = 1$ in (2.6), that

$$A(u^{(1)} - u^{(0)}) + f(u^{(0)})\Delta(u^{(1)} - u^{(0)}) + Q^{(0)}(u^{(1)} - u^{(0)}) \geqslant 0,$$

that is,

$$T^{(0)}(u^{(1)} - u^{(0)}) \geqslant 0.$$

This implies, since $T^{(0)}$ is inverse positive, that $u^{(1)} \geqslant u^{(0)}$. Assume that $u^{(k)} \geqslant u^{(k-1)}$ for some k. Using (2.6), one obtains

$$\begin{aligned} &A(u^{(k+1)} - u^{(k)}) + f(u^{(k)})\Delta u^{(k+1)} - f(u^{(k-1)})\Delta u^{(k)} \quad + Q^{(k)}(u^{(k+1)} - u^{(k)}) \\ &\quad = Q^{(k-1)}(u^{(k)} - u^{(k-1)}). \end{aligned}$$

That is,

$$\begin{aligned} &A(u^{(k+1)} - u^{(k)}) + f(u^{(k)})(\Delta u^{(k+1)} - \Delta u^{(k)}) + Q^{(k)}(u^{(k+1)} - u^{(k)}) \\ &\quad = -\{f(u^{(k)})\Delta u^{(k)} - f(u^{(k-1)})\Delta u^{(k)}\} + Q^{(k-1)}(u^{(k)} - u^{(k-1)}). \end{aligned}$$

Thus, $T^{(k)}(u^{(k+1)} - u^{(k)}) = \text{R.H.S.}$, where

$$\text{R.H.S.} = -\{f(u^{(k)})\Delta u^{(k)} - f(u^{(k-1)})\Delta u^{(k)}\} + Q^{(k-1)}(u^{(k)} - u^{(k-1)}).$$

Now, the aim is to show that R.H.S. $\geqslant 0$. Fix $i \in \{1, 2, \ldots, M\}$; $j \in \{1, 2, \ldots, M\}$. By an application of the mean value theorem, one obtains that

$$\begin{aligned} \{\text{R.H.S.}\}_{i,j} &= -\left(f\left(u_{i,j}^{(k)}\right)\Delta u_{i,j}^{(k)} - f_{i,j}(u^{(k-1)})\Delta u_{i,j}^{(k)}\right) + w_{i,j}^{(k-1)}\left(u_{i,j}^{(k)} - u_{i,j}^{(k-1)}\right) \\ &= \left(-f'(\xi_{i,j})\Delta u_{i,j}^{(k)} + w_{i,j}^{(k-1)}\right)\left(u_{i,j}^{(k)} - u_{i,j}^{(k-1)}\right), \end{aligned} \tag{2.10}$$

where $\xi_{i,j} \geqslant u_{i,j}^{(k-1)}$. Notice that

$$f'(\xi_{i,j}) = -\frac{1}{2}\frac{\Lambda}{\xi_{i,j}^{-3/2}}\Delta y \leqslant 0, \quad \text{whenever} \quad \xi_{i,j} \geqslant 0,$$

and

$$|f'(t_1)| \leqslant |f'(t_2)| \quad \text{if} \quad t_1 \geqslant t_2. \tag{2.11}$$

In the case

$$\frac{(1+\alpha)}{2}u_{i,j-1} - \left[\alpha u_{i,j}^{(k-1)} + \frac{(1-\alpha)}{2}u_{i,j+1}^{(k-1)}\right] \leqslant 0,$$

by construction, $w_{i,j}^{(k-1)} = 0$. So, from (2.11) and $\xi_{i,j} \geqslant u_{i,j}^{(k-1)}$, it follows that

$$w_{i,j}^{(k-1)} \geqslant |f'(\xi_{i,j})|\left\{\frac{(1+\alpha)}{2}u_{i,j-1} - \left[\alpha u_{i,j}^{(k-1)} + \frac{(1-\alpha)}{2}u_{i,j-1}^{(k-1)}\right]\right\}. \tag{2.12}$$

Hence, by applying (2.12) in (2.10), one obtains $\{\text{R.H.S.}\}_{i,j} \geqslant 0$. That is,

$$T^{(k)}(u^{(k+1)} - u^{(k)}) = \text{R.H.S.} \geqslant 0.$$

Now, since $T^{(k)}$ is inverse positive, it is easy to see $u^{(k+1)} \geqslant u^{(k)}$. The conclusion that $\{u^{(k)}\}$ is monotonic increasing follows by induction. Further, since $\bar{u} \geqslant u^{(k)}$, $k = 1, 2, \ldots$, it is clear that the sequence $\{u^{(k)}\}$ converges to a limit u^*, and u^* is the required solution of (2.3).

2.1. Selection of lower solution

For a convergent film, i.e., when $H_y(x, y) \leqslant 0$, $u = H^2(x, y)$ can be shown to be a lower solution (see the Appendix). This corresponds to the fact that $p \geqslant p_a$, the ambient pressure, for a convergent film. If the film is not a convergent one, then subambient pressure may develop. The study of the design performance characteristics of bearings requires numerical data for various Reynolds numbers. So if $\Lambda_1 < \Lambda_2 < \ldots < \Lambda_n < \ldots$ is a sequence of Reynolds numbers, it is natural to check whether the solution for Λ_{n-1} is a lower solution for Λ_n. For this, let v be the solution of (2.3) for Λ_{n-1}. Then,

$$Av + \frac{\Lambda_{n-1}}{\sqrt{v}}\Delta y \Delta v = b.$$

Consider the problem (2.3) with Λ_n. Now, replacing u by v, one obtains that

$$Av + \frac{\Lambda_n}{\sqrt{v}}\Delta y \Delta v = b.$$

So, v is a lower solution of (2.3) for Λ_n if

$$\frac{\Delta y \Delta v}{\sqrt{v}}(-\Lambda_{n-1} + \Lambda_n) \leqslant 0.$$

That is, if $\Delta v \leqslant 0$.

Since v is already known, this condition can be easily verified by computation. If this holds, then v, the solution for Λ_{n-1}, is a lower solution for Λ_n. When this is not true, further increase of Λ may not increase the pressure distributions and hence the work load. Notice that when $\Delta v \geqslant 0$, v is an upper solution of (2.3) for Λ_n.

2.2. Selection of upper bound

Consider the film shapes (1.4) and (1.7) for a complete discussion. Similar ideas hold for other geometries also (see also the Appendix). For a convergent film, $\bar{u} = \max_y[H^2(y)] = H^2(0)$. By the above proof, for convex crowning ($\beta \geqslant 0$), the solution $u^* \leqslant \bar{u}$. This means that $u^* = (PH)^2 \leqslant \bar{u} = H^2(0)$. That is, $p(x) \leqslant \bar{p}(x) = H(0)/H(x)$. It is interesting to note that this $\bar{p}$ has been used in the literature (for example, see [1,4]) as the limiting solution of (1.3) for Λ tends to ∞. This limiting solution applies to convex as well as concave sliders. Because of this physical reason, $\bar{u}$ can be taken as $H^2(0)$ in the numerical procedure for concave crowning also. Note that the rate of convergence depends on the upper-bound estimate $\bar{u}$ of $u^{(k)}$, $k = 1, 2, \ldots$. If $\bar{u}$ is large, then the rate of convergence will be slow. In fact, the $\bar{u}$ considered above is an over-all common bound which may not be a good one for an individual $u^{(k)}$. So, in what follows, a procedure is given to construct $\bar{u}^{(k)}$, an upper estimate to each $u^{(k)}$, depending on the previous iterate $u^{(k-1)}$.

Denote $\hat{g}^{(k-1)}(i,j) = s(i,j) + \alpha f_{i,j}(u^{(k-1)})$. For simplicity, dropping the superscript $(k-1)$ and the index (i,j) in $\hat{g}$, g_1, g_2, g_3 and g_4 define

$$c_{i,j} = \max\left\{0, \frac{-\left[\hat{g}u_{i,j}^{(k-1)} + g_1 u_{i,j-1}^{(k-1)} + g_2 u_{i,j+1}^{(k-1)} + g_3 u_{i-1,j}^{(k-1)} + g_4 u_{i+1,j}^{(k-1)}\right]}{\hat{g} + g_1 + g_2 + g_3 + g_4 + \tau}\right\},$$

where $\tau > 0$. Let $c = \max_{i,j}\{c_{i,j}\}$. Now,

$$\hat{g}\left[u_{i,j}^{(k-1)} + c\right] + g_1\left[u_{i,j-1}^{(k-1)} + c\right] + g_2\left[u_{i,j+1}^{(k-1)} + c\right] + g_3\left[u_{i-1,j}^{(k-1)} + c\right]$$

$$+ g_4\left[u_{i+1,j}^{(k-1)} + c\right] + \tau c \geqslant 0.$$

Letting $w_{i,j}^{(k-1)} \geqslant \tau > 0$, and $v = u^{(k-1)} + c$, one gets

$$\hat{g}v_{i,j} + g_1 v_{i,j-1} + g_2 v_{i,j+1} + g_3 v_{i-1,j} + g_4 v_{i+1,j} \quad + w_{i,j}^{(k-1)} v_{i,j} \geqslant w_{i,j}^{(k-1)} u_{i,j}^{(k-1)},$$

that is,

$$T^{(k-1)}v \geqslant Q^{(k-1)}u^{(k-1)} + b = T^{(k-1)}u^{(k)}.$$

Thus, $v \geqslant u^{(k)}$. Notice that this estimate holds both for convex as well as concave sliders. Hence we have upper estimates $\bar{u}_{i,j}$ and $v_{i,j}$ for $u_{i,j}^{(k)}$. The minimum of these two is to be chosen in the computation of $w_{i,j}^{(k-1)}$ for our numerical scheme. Observe that if $\bar{u}_{i,j}$ is used, then there is no restriction on the minimum positive value of $w_{i,j}^{(k-1)}$. In the other case, $w_{i,j}^{(k-1)} \geqslant \tau > 0$. Typically, τ can be chosen as 0.1 or 0.01.

We note that the above *a priori* estimates for $\Delta u^{(k)}$ may be large when the film-thickness ratio is large. This, in turn, may affect the rate of convergence. Rigorous estimates of $\Delta u^{(k)}$, in general, will be more expensive. So we consider the approximation $\Delta u^{(k)} \approx$

$\Delta(u^{(k-1)}+z)$, where $z=u^{(k-1)}-u^{(k-2)}$. Notice that for the first iterate in (2.6), $Q^{(k)}$ can be zero and still $u^{(1)}\geqslant u^{(0)}$. This estimate seems to be a reasonable one. In fact we experimented with many examples and found this approach to be very successful. For example, even for the high eccentricity $\epsilon=19$ (film shape (1.7) with $a=0$) and $\Lambda=500$, it took only 8 iterations to get monotonic convergence, starting from the lower solution $u=H^2(1,\epsilon,a)$.

3. Numerical results and discussion

Once the pressure distribution is known, the dimensionless workload is given by

$$W=2\int_0^1\int_0^{L'/2}[P(x,y)-1]\,\mathrm{d}x\,\mathrm{d}y, \tag{3.1}$$

and the y coordinate of the center of pressure is

$$y_c=\frac{2}{W}\int_0^1\int_0^{L'/2}y[P(x,y)-1]\,\mathrm{d}x\,\mathrm{d}y.$$

Because of symmetry, the x coordinate is, of course, zero. In the case of a one-dimensional

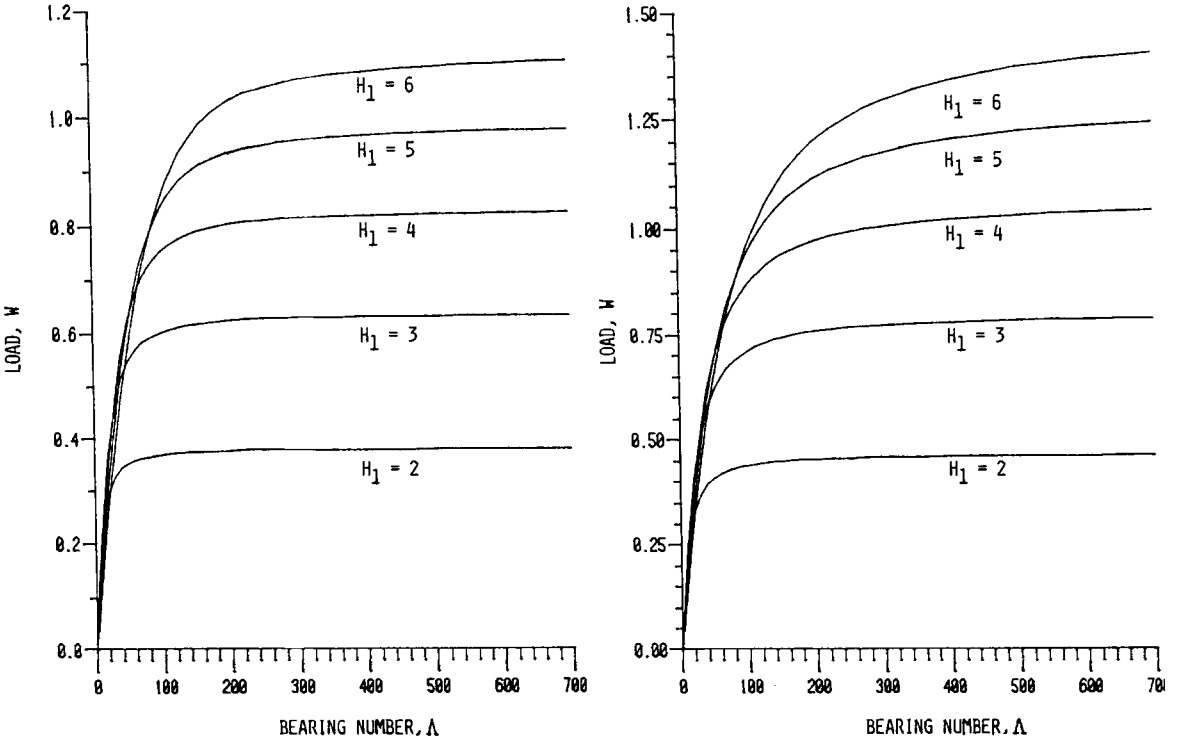

Figure 2. Effect of film-thickness ratio and bearing number on bearing load for infinitely long plane-wedge films ($a=0$ in (1.7)).

Figure 3. Effect of film-thickness ratio and bearing number on bearing load for parabolic films (1.7) with $a=0.5$.

problem (for infinite sliders), work load and center of pressure are computed using Simpson's rule. For finite sliders, the above integrals are computed using the I.M.S.L. subroutine DBCQDU. This routine computes an approximate double integral to a given table of data using a natural bicubic spline interpolant. Figures 2 and 3 illustrate the effect of bearing number and film-thickness ratio upon isothermal load for infinitely long inclined pad and curved slider bearings. Figures 4 and 5 represent the effect of curvature upon load for infinitely long curved sliders. In Figs. 6 and 7, notice that the pressure peaks near the trailing edge for increased Reynolds numbers. Numerical values of dimensionless load and center of pressure are listed in Table 1 for finite, cylindrical sliders with different curvatures. Notice from Table 1 that convexity increases and concavity decreases the work load. Table 2 gives the work loads for plane sliders having film-thickness ratio $H_1 = 3$ and length ratios $L/B = 1$, and $L/B = \infty$, respectively. From this table one can see the load-capacity reduction due to side flow. For high Reynolds numbers, the side flow rate is decreased, and the load values for the finite slider approaches that of the infinite slider. The stopping criterion used is $|u^{(k)} - u^{(k-1)}| \leqslant E$, $E = 10^{-3}$. The results computed for $E = 10^{-4}$ show only slight improvement, less than 0.02%, over those obtained for $E = 10^{-3}$. For infinite sliders, the grid size $\Delta x = 0.01$ is used for large Reynolds numbers. A larger grid size $\Delta x = 0.05$ is recommended for small Reynolds numbers. For large

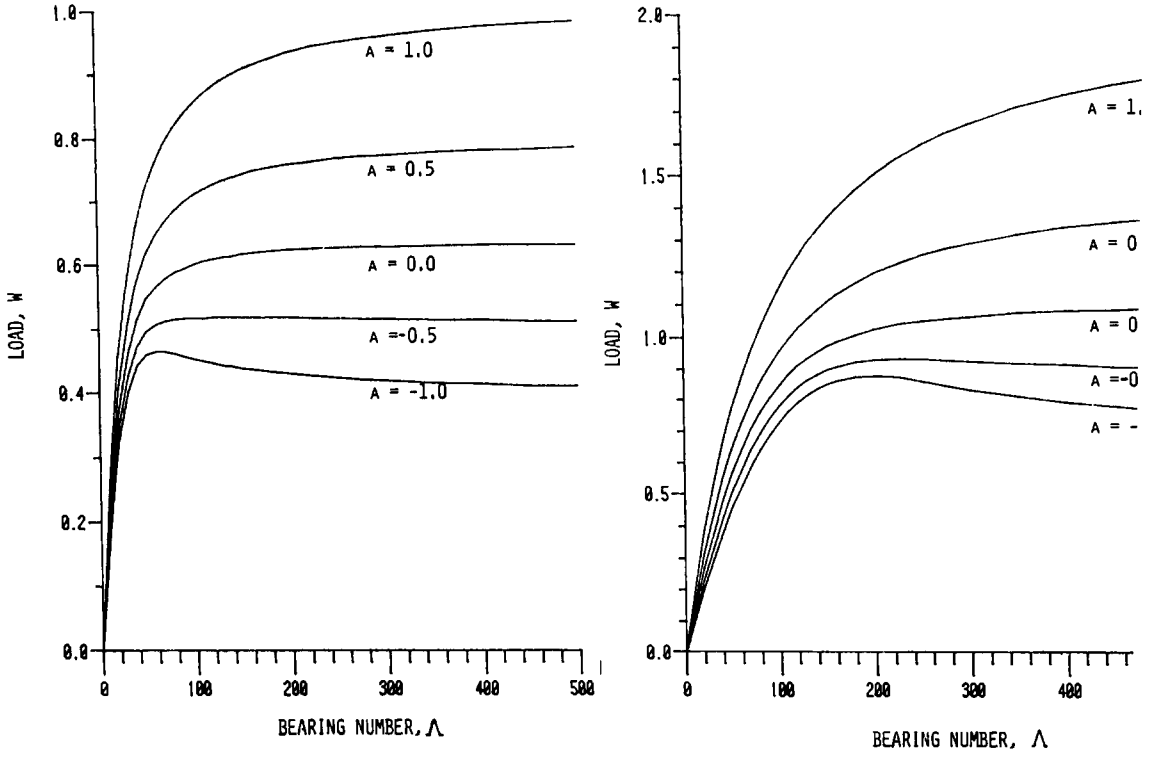

Figure 4. Effect of the parameter a and bearing number on bearing load for parabolic films (1.7) with eccentricity $\epsilon = 2$.

Figure 5. Effect of the parameter a and bearing number on bearing load for parabolic films (1.7) with eccentricity $\epsilon = 5$.

values of Λ, as expected, finier grid size helps to reduce the discretization error. Sometimes the improvement in accuracy may not be that much significant. For example, when $a = 0$ and $\epsilon = 1$, the work load obtained with $\Delta x = 0.01$ is 0.3820, and it is 0.3837 for $x = 0.005$. Thus, the difference is only about 0.4%.

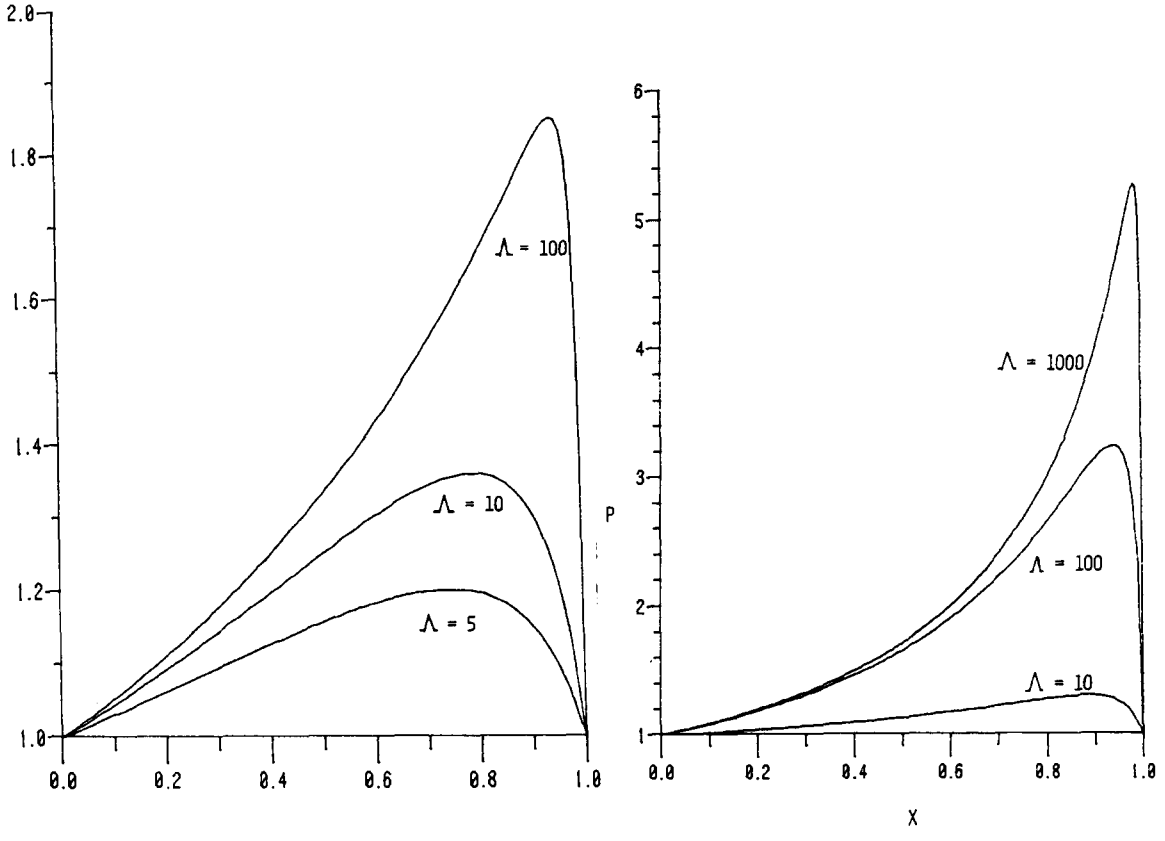

Figure 6. Pressure profiles for infinitely long plane-wedge gas films ($a = 0$ in (1.7)) having film thickness ratio $H_1 = 2$.

Figure 7. Pressure profiles for infinitely long plane-wedge gas films ($a = 0$ in (1.7)) having film thickness ratio $H_1 = 6$.

Table 1. Film shape (1.4) with $H_1 = 3$.

Λ	Work load			Center of pressure; y-coordinate		
	$\beta = 0.5$	$\beta = 0.1$	$\beta = -0.1$	$\beta = 0.5$	$\beta = 0.1$	$\beta = -0.1$
25	0.3122	0.2366	0.2114	0.6372	0.6887	0.6846
100	0.6408	0.4652	0.4048	0.6629	0.6968	0.7175
200	0.7617	0.5382	0.4584	0.6687	0.7021	0.7236
300	0.8140	0.5693	0.4809	0.6712	0.7043	0.7259
500	0.8732	0.6088	0.5124	0.6767	0.7106	0.7328
700	0.8989	0.6243	0.5236	0.6779	0.7115	0.7337
1000	0.9208	0.6378	0.5335	0.6788	0.7123	0.7344

In the one-dimensional case, at each iteration, the resulting linear system is solved using the standard tridiagonal algorithm. For finite sliders, $\Delta x = 0.025$, $\Delta y = 0.025$ are chosen for $\Lambda < 300$, and for $\Lambda \geqslant 300$, $\Delta x = 0.025$, $\Delta y = 0.01$ are used. To solve the resulting linear system at each iteration, a successive over-relaxation scheme is used. As far as convergence is concerned, no difficulty is experienced with this scheme. For our computations, ω, the overrelaxation parameter, is chosen near 1 $(1 - 1.25)$ when $\Lambda \geqslant 100$. With increased grid refinement, one may have to increase ω slightly. For small Reynolds numbers ($\Lambda < 100$), ω is taken as 1.75. This scheme is notably inexpensive. It does not require any matrix inversion and very little storage space is needed. In contrast to this, the column method [1], pp. 621-623, requires (at each step) for an $N \times M$ mesh, N inversions of an $M \times M$ matrix and the storage of all these quantities for further multiplications.

The following schemes are the most common ones in practice to solve (2.1). Let

$$Su \equiv -H(x, y)\left(\frac{\partial^2 u}{\partial x^2} + \frac{\partial^2 u}{\partial y^2}\right) + \frac{\partial Y}{\partial x}\frac{\partial u}{\partial x} + \frac{\partial Y}{\partial y}\frac{\partial u}{\partial y} + 2\left(\frac{\partial^2 H}{\partial x^2} + \frac{\partial^2 H}{\partial y^2}\right)u.$$

Then, for $k = 0, 1, 2, \ldots$, the Picard (natural linearization) scheme [3] is

$$Su^{(k+1)} + \frac{\Lambda}{\sqrt{u^{(k)}}}\frac{\partial u^{(k+1)}}{\partial y} = 0,$$

and the Newton-Raphson scheme [2] is

$$Su^{(k+1)} + \frac{\Lambda}{\sqrt{u^{(k)}}}\frac{\partial u^{(k+1)}}{\partial y} - \frac{\Lambda}{2(u^k)^{3/2}}\left(\frac{\partial u^{(k)}}{\partial y}\right)(u^{(k+1)} - u^{(k)}) = 0.$$

In both these schemes, centered differences are used. These methods are hit-or-miss type. That is, convergence for these schemes is unpredictable and it depends on the grid, and the parameters Λ and H_1. Also, since centered differences are used for all the derivatives, these schemes becomes numerically unstable for large Λ. This numerical instability often leads to overshooting the answeres. Thus, even when they converge, the computed values are unreliable. For example, consider an infinitely long plane slider. In this case (see the Appendix) $u = H^2(0)$ is an upper solution for (2.1). That is, $P(y) = H(0)/H(y)$ is an upper solution for the pressure distribution. This $\bar{P}$, when $H_1 = 1.1$, gives the work load $w_\infty = 0.0484$. So, this w_∞ is an upper bound for this geometry for any Λ. This upper bound is also known [4] as the limiting load for $\Lambda \to \infty$. However, for $\Lambda = 200$ with $\Delta y = 0.05$,

Table 2. Film shape (1.4) with $H_1 = 1 + \epsilon = 3$, $\beta = 0$.

Λ	50	100	200	300	500	700	1000
Work load							
$\frac{L}{B} = 1$	0.3367	0.4332	0.4963	0.5229	0.5487	0.5644	0.5736
$\frac{L}{B} = \infty$	0.5473	0.6028	0.6264	0.6313	0.6351	0.6405	0.6415

the above two schemes [2,3] compute the work load as 0.0509, Notice that this value is above the upper-bound level. This example shows the overshooting of these schemes. This overshooting continues to grow as Λ increases. On the other hand, for the same grid size and Λ, our scheme calculates the workload as 0.0467. Since a weighted upwind-difference form is used for the first-order derivative in the nonlinear part, our scheme is numerically stable independent of Λ, eccentricity and grid. Further, this gives guaranteed convergence. As a second example consider the film shape (1.7) with $a = 0$, $\epsilon = 19$. For $\Lambda = 500$, both the above schemes do not converge. However, our scheme converges. The starting solution is taken as $u = H^2(y)$ which corresponds to the ambient pressure $P \equiv 1$. Results are listed in Table 3.

Failures of the Picard method have been reported at several places in the literature [1,2,3]. In [1], pp. 583, it is noted that, "typically no convergence is obtained for local values of Λ of about 50" (film shape is not specified). In [2], Newton-Raphson scheme is proposed as a better choice. However, because centered differences are used, it is found (for the example discussed) that this method becomes numerically unstable faster than Picard as Λ increases. In conclusion, it is clear that our scheme is more powerful in solving extreme situations (i.e., very large Λ and very large eccentricity).

It is known that asymptotic methods give good results for small eccentricity [4]. But, as noted in [4], these methods give poor results for moderate or large values of eccentricity. The asymptotic load value for high Λ is obtained from the limiting pressure distribution (upper solution). Depending upon Λ, an approximate correction is offered to the limiting load value W_∞. For an infinite slider (1.7), the study can be found in [4], and for finite sliders, see [5,6] and the references therein. In order to check the validity of our results some of our results are listed in Table 4 below along with those obtained by asymptotic methods [4] for small eccentricity (film shape (1.7)).

This table shows good agreement of our results with those already known. As noted before, the asymptotic analysis may not give good results for moderate or large values of eccentricity. According to [4], an explanation for this is that the coefficient of $1/\Lambda^2$ in the asymptotic expansion of P is very large when ϵ is not small. Notice that the analysis takes into account only up to the first-order term in the series expansion of P in negative powers of Λ. For example, for $a = 0.5$, $\epsilon = 5$, and $\Lambda = 100$, the computed value of work load W is 0.955. But the asymptotic method [4] gives the value $W = 0.855$. Thus, the error in

Table 3. Film shape (1.7) with $a = 0$, $\epsilon = 19$; grid size $\Delta y = 0.01$, $\Lambda = 500$.

Picard [3]	No convergence	–
Newton [2]	No convergence	–
New scheme	Convergence	Work load = 1.1205

Table 4.

Λ	$a = 0, \epsilon = 1$		$a = 0, \epsilon = 2$	
	Computed value	Asymptotic value	Computed value	Asymptotic value
100	0.3707	0.3712	0.6028	0.6079
1000	0.3837	0.3847	0.6415	0.6439

asymptotic value is about 11.7%. As a second example, let $a = 0.00$, $\epsilon = 10$ in (1.7), and $\Lambda = 100$. The asymptotic value [4] is 1.03768, and the computed value is 0.6045. Hence, the error in asymptotic value is about 70%. DiPrima [4] has noted that if the two-term asymptotic results are correct at $\Lambda \cong 33.3$, it follows that at this value of Λ the maximum of W will occur for $a = -1$ and $\epsilon = 2$. But, Fig. 4. reveals that actually the maximum of W occurs for $\Lambda \cong 65$ when $a = -1$ and $\epsilon = 2$. Figure 4 presents more accurate curves than those given in fig. 4 of [4] (Fig. 3.8.4 in [1], pp. 137). Moreover, calculations of other data like pressure distributions, frictional characteristics, etc., are not straightforward with asymptotic analysis. So, for a complete and accurate study of film characteristics, one has to adopt numerical procedures. Some analytical investigations have been reported in [7,8]. There, using the transformation $u = p^2$ for the Reynolds equation, they have obtained a lower bound (lower solution) and an upper bound (upper solution) for the pressure for a one-dimensional film shape. The general purpose of the monotone method in [7] is to prove existence of minimal and maximal solutions. This can also be used to obtain analytical bounds. But, since the Nagumo constant involved there is too big (construction is also complicated), the method cannot be applied for practical computations of pressure distributions. Notice also that the method [7] does not take care the constant to be updated at each step which is crucial for faster convergence. Further, the treatment [7] is restricted to the one-dimensional case only. It is known that the numerical treatment of a nonlinear convection-diffusion equation of the form (2.1) presents serious difficulties because of the nonlinear term containing the first derivative. When the first-order term is dominant (the most interesting practical case) the problem becomes a singularly perturbed one. For mildly nonlinear problems (that is, when the first-order term is not present), monotone iterative methods are known [11,12]. Numerical schemes for a general nonlinear convection-diffusion equation with turning points and FORTRAN programs for the results presented in this paper are given in [13].

Numerical values in Tables 1–4 have been computed using an IBM 4341 computer at the University of Texas at Arlington. For Figures 2-7, computer runs have been made on a DEC-20, and the results are directly graphed using an Interactive Graphing Package (IGP) available at the University of Texas at Arlington. In terms of c.p.u. time, this scheme is very economical. As an example, for the film shape (1.7) with $a = 0$, $\epsilon = 1$, the c.p.u. time on DEC-20 is 3.9 seconds for 30 values of Λ ranging from 10 to 700.

Conclusion

An inexpensive, accurate, and reliable numerical scheme is presented for gas-lubricated slider bearings. Convergence of our scheme is proved independent of Reynolds numbers and film-thickness ratios. The scheme is numerically stable for all grid choices. Comparisons are made with other existing techniques, numerical as well as asymptotic. The present scheme is more powerful in handling the extreme situations, viz., high eccentricities and large Reynolds numbers.

Acknowledgement

This work is based in part on a portion of the author's doctoral thesis which was submitted in partial fulfilment of the requirements for the degree of Doctor of Philosophy

at University of Texas-Arlington (1984). The author would like to express his appreciation to the thesis committee.

Appendix

An off-diagonally nonpositive matrix $A \in L(R^n)$ is referred as a Z-matrix, and an inverse positive Z-matrix is called an M-matrix.

THEOREM A.1. [9]: *A Z-matrix $A \in L(R^n)$ is an M-matrix if and only if there exists a vector $z \in R^n$ such that $z \geqslant 0$, $Az \geqslant 0$, and $\sum_{j=1}^{i} a_{ij} z_j > 0 (i = 1, 2, \ldots, n)$.*

For the proof of our main results, the test vector z can be taken as e, $e_i = 1$ $(i = 1, 2, \ldots, n)$. Next, the definition of a lower solution and an upper solution are given. For simplicity, express the elliptic equation (2.1) as

$$\nabla^2 u = F\left(x, y, u, \frac{\partial u}{\partial x}, \frac{\partial u}{\partial y}\right), \tag{A.1}$$

where $\nabla^2 = -(\partial^2/\partial x^2 + \partial^2/\partial y^2)$. The boundary conditions in (2.1) are denoted by

$$Bu = \phi(x, y). \tag{A.2}$$

A function $\underline{u}$ is said to be a lower solution of (A.1)–(A.2) if it satisfies

$$\nabla^2 \underline{u} \leqslant F\left(x, y, \underline{u}, \frac{\partial \underline{u}}{\partial x}, \frac{\partial \underline{u}}{\partial y}\right), \quad B\underline{u} \leqslant \phi(x, y). \tag{A.3}$$

A function $\bar{u}$ is said to be an upper solution of (A.1)–(A.2) if it satisfies (A.3) with inequalities reversed. Now, it can be verified that $\underline{u} = H^2(x, y)$ is a lower solution, provided the film is convergent, i.e. $\partial H/\partial y \leqslant 0$. If $\partial^2 H/\partial y^2 \leqslant 0$, then $\underline{u}(x) = \min\{H^2(x, 0), H^2(x, 1)\}$ is a lower solution. For a divergent film, $\bar{u} = H^2(x, y)$ is an upper solution. If the film is having nonnegative crown height in the sliding direction, then $\bar{u}(x) = \max\{H^2(x,)), H^2(x, 1)\}$ is an upper solution.

References

[1] W.A. Gross, (Editor), *Fluid film lubrication*, John Wiley and Sons, Inc., New York (1980).

[2] R. Coleman and A.D. Snider, Linearization for numerical solution of the Reynolds equation, *ASME Journal of Lubrication Technology* 91 (1969) 506–507.

[3] V. Castelli and J. Pirvics, Review of numerical methods in gas bearing film analysis, *ASME Journal of Lubrication Technology* 90 (1969) 777–792.

[4] R.C. DiPrima, Higher order approximations in the asymptotic solution for the Reynolds equation for slider bearings at high bearing numbers, *ASME Journal of Lubrication Technology* 91 (1969) 45–51.

[5] R.C. DiPrima and J.A. Schmitt, Asymptotic methods for a general finite width gas slider bearing, *ASME Journal of Lubrication Technology* 100 (1978) 254–260.

[6] J.J. Shepard and R.C. DiPrima, Asymptotic analysis of a finite gas slider bearing of narrow geometry, *ASMe Journal of Lubrication Technology* 105 (1983) 491–495.

[7] J.C. Chandra and P.W. Davis, A monotone method for quasilinear boundary value problems, *Arch. Rational Mech. Anal.* 54 (1974) 257–266.

[8] J.C. Chandra and P.W. Davis, Some analytic observations on gas lubricated slider bearing, *ASME Journal of Lubrication Technology* 104 (1982) 271–274.

[9] J. Schroder, *Operator inequalities*, Academic Press, Inc., New York (1980).

[10] W.J. Steinmetz, On a nonlinear singular perturbation boundary value problem in gas lubrication theory, *SIAM J. Appl. Math.* 26 (1974) 816–827.

[11] D. Greenspan and S.V. Parter, Mildly nonlinear elliptic partial differential equations and their numerical solution II. *Numer. Math.* 7 (1965) 129–146.

[12] J.M. Ortega and W.C. Rheinboldt, *Iterative solution of nonlinear equations in several variables*, Academic Press, Inc., New York (1970).

[13] M.C. Pandian, Numerical studies of nonlinear systems and quasilinear boundary value problems with application to gas lubricating films, *Ph.D. Thesis*, Univ. of Texas, Arlington (1984).